DNA-templated nanoantennas for single-molecule detection at elevated concentrations

Guillermo P. Acuna
Phil Holzmeister
Friederike M. Möller
Susanne Beater
Birka Lalkens
Philip Tinnefeld

DNA-templated nanoantennas for single-molecule detection at elevated concentrations

Guillermo P. Acuna, Phil Holzmeister, Friederike M. Möller, Susanne Beater, Birka Lalkens, and Philip Tinnefeld
Technische Universität Braunschweig, Physical and Theoretical Chemistry—NanoBioScience, Hans-Sommer-Strasse 10, 38106 Braunschweig, Germany

Abstract. The dynamic concentration range is one of the major limitations of single-molecule fluorescence techniques. We show how bottom-up nanoantennas enhance the fluorescence intensity in a reduced hotspot, ready for biological applications. We use self-assembled DNA origami structures as a breadboard where gold nanoparticle (NP) dimers are positioned with nanometer precision. A maximum of almost 100-fold intensity enhancement is obtained using 100-nm gold NPs within a gap of 23 nm between the particles. The results obtained are in good agreement with numerical simulations. Due to the intensity enhancement introduced by the nanoantenna, we are able to perform single-molecule measurements at concentrations as high as 500 nM, which represents an increment of 2 orders of magnitude compared to conventional measurements. The combination of metallic NPs with DNA origami structures with docking points for biological assays paves the way for the development of bottom-up inexpensive enhancement chambers for single-molecule measurements at high concentrations where processes like DNA sequencing occur. © 2013 Society of Photo-Optical Instrumentation Engineers (SPIE) [DOI: 10.1117/1.JBO.18.6.065001]

1 Introduction

Single-molecule fluorescence studies provide a number of significant advantages over ensemble measurements. Examples are the sensitivity for subpopulations, observation of kinetics without synchronization, or molecule sorting with respect to parameters such as fluorescence resonance energy transfer. Conventional single-molecule spectroscopy techniques are limited to observe a single molecule in a diffraction-limited focus of submicrometer dimensions, which translates into a concentration maximum in the nanomolar range. Unfortunately, most significant biological processes such as, for example, DNA sequencing, require concentrations orders of magnitude higher in the micro- or even millimolar range.[1,2] In order to overcome the concentration limitation of optical single-molecule techniques, two nanophotonic approaches were recently pursued. The first one relies on the employment of so-called zero mode wave guides, which consist of circular holes of 50 to 200 nm diameter in a metal layer deposited on a glass slide. Due to the subwavelength nature of the apertures, light cannot propagate through the circular hole and it is confined to a reduced volume in the zeptoliter range.[3] This technique has enabled the study of enzymatic reactions at high substrate concentrations.[4] The second approach consists of exploiting the plasmonic properties of metallic nanostructures to create nanoantennas that focus the incoming light to a reduced volume, termed hotspot, beyond the diffraction limit.[5,6] In this way, single-molecule measurements at concentrations as high as 1 μM were demonstrated.[7] Despite this impressive progress, both approaches suffer from several shortcomings.

Address all correspondence to: Guillermo P. Acuna, Technische Universität Braunschweig, Physical and Theoretical Chemistry—NanoBioScience, Hans-Sommer-Strasse 10, 38106 Braunschweig, Germany. Tel: +49 531 391 7377; Fax: +49 531 391 5334; E-mail: g.acuna@tu-bs.de

Demanding nanolithography is required in an intrinsic serial fabrication process and the molecules of interest can only be randomly placed within the aperture or hotspot yielding heterogeneous signals and even strong quenching of the single fluorophores in close proximity to the metallic structures.

In this contribution, we show how these difficulties can be overcome by employing the recently developed DNA-origami technique.[8] We build a nanopillar shaped DNA origami structure where one or two metallic nanoparticles (NPs) can be placed[9] with nanometer precision forming a nanoantenna monomer and dimer, respectively. Furthermore, a single fluorophore is positioned at the hotspot of the nanoantenna. Due to the wet chemical synthesis of the structures, the fabrication process is intrinsically parallelized.

2 Theory and Numerical Simulations

Away from saturation, the fluorescence intensity I of a dye can be expressed as[10]

$$I = k_{ex} \times k_{rad}/(k_{rad} + k_{nrad}), \qquad (1)$$

where k_{ex}, k_{rad}, k_{nrad} are the excitation, radiative and nonradiative rates, respectively. k_{ex} is proportional to the electric field intensity (electric field square).[11] $k_{rad}/(k_{rad} + k_{nrad})$ can be regarded as the quantum yield of the fluorophore and refers to the emission process, with the fluorescence lifetime $\tau_f = 1/(k_{rad} + k_{nrad})$. When a dye is placed close to a metallic structure, all rates are generally affected, yielding an enhancement or reduction of the fluorescence intensity depending on several factors like the geometry and size of the particle as well as the distance between the dye and the particle surface.[6,10]
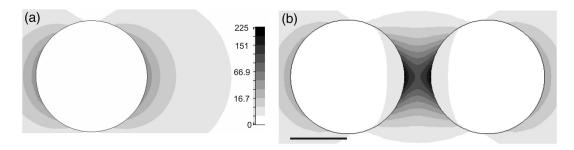
Fig. 1 Numerical simulation of electric field intensity (E^2) for a monomer (a) and dimer (b) for 100 nm diameter gold NPs and an interparticle spacing of 23 nm (dimer). The incoming light was horizontally polarized at a wavelength of 640 nm. Scale bar is 50 nm.

In order to study how the interaction of a fluorophore with a metallic NP affects the excitation rate, it is sufficient to calculate the local electric field intensity at the dye position. Upon illumination, metallic NPs get polarized[12,13] and thus the electric field intensity in the vicinity of the NP arises from two different components, the incoming electric field and the electric field due to the polarized NP. Figure 1(a) shows a numerical simulation of the electric field intensity enhancement at the equator plane of a 100-nm diameter gold NP at a frequency of 640 nm. Due to the electromagnetic coupling between metallic particles, an NP dimer will yield a higher electric field intensity enhancement at the gap between the NPs. The electric field intensity pattern at the equator plane of a dimer is included in Fig. 1(b), again for

100-nm diameter NPs with an interparticle spacing of 23 nm at the same excitation frequency.

Besides the number and size of the NPs, the electric field intensity enhancement strongly depends on the interparticle spacing. A stronger enhancement occurs for NPs in close proximity,[6] see Fig. 2(a) for a numerical simulation of the electric field intensity enhancement at the center of the gap between the NP dimer.

As previously stated, the presence of NPs in the vicinity of a fluorophore not only alters the excitation rate due to the change in the local electric field intensity but also modifies the emission properties. The NPs can couple to the fluorophore and act as an antenna mediating the radiation and thus increase the radiative
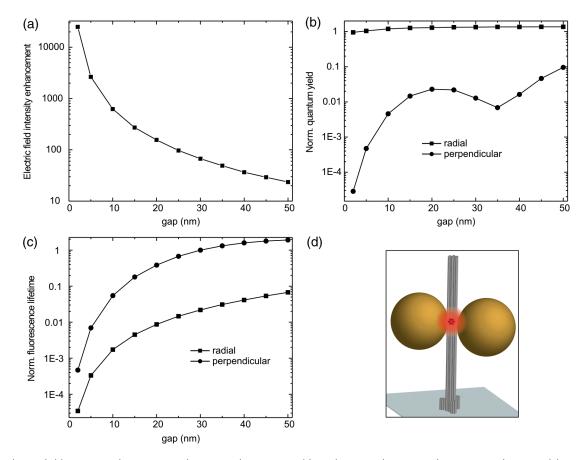

Fig. 2 (a) Electric field intensity enhancement at the center of a 100 nm gold NP dimer at a frequency of 640 nm as a function of the gap size. The incoming electric field is polarized along the line connecting the NPs. Relative change in quantum yield (b) and fluorescence lifetime (c) at the center of a NP dimer for a fluorophore placed with a radial and perpendicular orientation and an intrinsic quantum yield of 0.65 at a frequency of 669 nm. (d) Sketch of the DNA origami structure, the nanoparticles forming the nanoantenna dimer are included as well as the fluorophore placed at the hotspot.

rate but also offer more paths to decay without photon emission leading to an enhancement of the nonradiative rate.[5,13] As a result, the relative change in quantum yield of a fluorophore close to NPs can be smaller or greater than one showing a strong dependence with the intrinsic quantum yield of the fluorophore. Figure 2(b) shows a numerical simulation of the relative change of the quantum yield of a fluorophore with an intrinsic quantum yield of 0.65 placed at the center of the NP dimer for a radial and perpendicular orientation at a frequency of 669 nm as a function of the gap size. For the radial orientation, the quantum yield is slightly enhanced, whereas for the perpendicular orientation, the quantum yield is reduced. The relative change in fluorescence lifetime is included in Fig. 2(c). At the center of the dimer, the fluorophore couples in a more efficient way to the dimer in the radial orientation and therefore the emission process is facilitated yielding a reduction in the fluorescence lifetime, whereas for the perpendicular orientation, this effect is less pronounced.

3 Materials and Methods

Based on the results of Sec. 2, we designed a DNA origami nanopillar capable of hosting two 100 nm gold NPs with a gap size of 23 nm, see Fig. 2(d). Although smaller gap sizes yield a greater fluorescence enhancement, our choice is a compromise between strong fluorescence enhancement and sufficient space for accommodation of a biomolecular assay in the gap between the particles. The DNA origami nanopillar has been previously characterized[14,15] and was folded from one M13mp18-derived scaffold strand and 207 staple strands. The structure consists of a 15-nm diameter 12-helix bundle with a length of 220 nm and three extra 6-helix bundles on the base, leading to a base diameter of ~30 nm. Selective

immobilization of the DNA origami nanopillar on coverslips coated with biotinylated bovine serum albumin and neutravidin was achieved by modifying 15 staple strands at the base with biotin. The structure was further modified to include an ATTO647N fluorophore and six capturing strands (A15, three per NP) at the half height of the nanopillar (further details are included in Ref. 14). ATTO647N has an intrinsic quantum yield of 0.65 and an emission peak at approximately 669 nm. Au NPs of 100 nm were functionalized[16] with the complimentary sequence and added to the previously immobilized DNA origami nanopillar structures. This hybridization procedure minimizes sample consumption and avoids aggregation.[17] Additionally, by controlling the incubation time, the yield of dimers, monomers, and nanopillars without particles can be controlled for an internal reference.

The ATTO647N fluorophores were excited using a 640 nm pulsed laser (80 MHz, LDH-D-C-640, Picoquant, Berlin, Germany) on a custom-built confocal setup based on an Olympus IX-71 inverted microscope with a high NA objective (UPlanSApo60XO, 1.35 NA, Olympus, Tokyo, Japan). The excitation light was circularly polarized after a quarter-wave-plate (Thorlabs, Newton, NJ) and separated spectrally from the fluorescence signal with a dichroic beam splitter and a band-pass filter (z532/633, ET 700/75 m, Chroma, Irvine, CA). Emitted photons were detected by an avalanche photo diode (τ-SPAD-100, Picoquant, Berlin, Germany) and a PC card for time-correlated single-photon counting (SPC-830, Becker & Hickl, Berlin, Germany) to determine the fluorescence intensity and lifetime. Phosphate-buffered saline was used as a solvent because it is known that ATTO647N exhibits pronounced blinking in this buffer.[18] This blinking directly visualizes single-molecule detection.
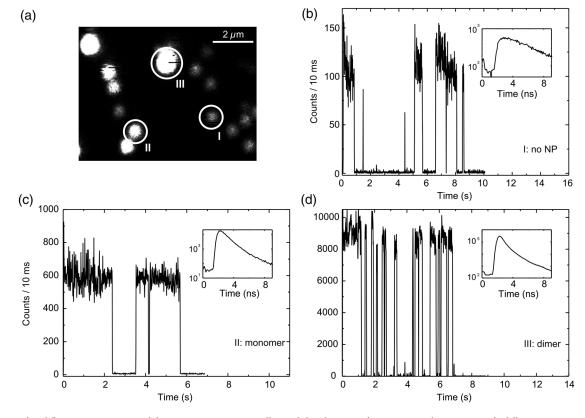

Fig. 3 (a) Confocal fluorescence image of the DNA origami nanopillar with binding sites for two NPs. Three spots with different intensities are highlighted: I (no NP), II (monomer), and III (dimer). (b to d) Corresponding fluorescence transients together with their fluorescence decays (insets).

4 Results and Discussion

A typical fluorescence confocal image is presented in Fig. 3(a). Spots of a broad range of intensities can be observed together with some fluorescence intermittencies, which indicate the presence of a single fluorescent dye for even the brightest spots. From the scan image, three spots with different intensities including a dim spot, a spot with intermediate intensity, and a bright spot were selected and labeled as I, II, and III, respectively. The corresponding fluorescence transients are included in Fig. 3(b)–3(d). In all three cases, single-step photobleaching confirmed the presence of a single fluorophore and revealed markedly different average intensities of 11, 60, and 900 kHz, respectively. Further insight into the experiment results can be gained by studying the fluorescence lifetime of the selected transients [see inset in Fig. 3(b)–3(d)]. For the dim transient in Fig. 3(b), a fluorescence lifetime of 4.55 ns is obtained, characteristic of ATTO647N. For the other two cases, a lifetime of 0.97 and 0.50 ns is extracted. As discussed in Sec. 1, the shortening of the fluorescence lifetime indicates the interaction of the fluorophore with the metallic structure. We therefore assign the dim transient to a nanopillar structure without NPs, the intermediate one to a nanopillar with one NP (monomer), and the bright transient to a nanopillar with two NPs (dimer). This observation was further supported by comparison with experiments where the nanopillar structures were only equipped with three capturing strands, capable of binding only one NP.[14]

The results obtained are in good agreement with the simulations presented in Sec. 1 and indicate that the dimer structure yields fluorescence intensity enhancement of almost 2 orders of magnitude at the hotspot.

Once the fluorescence enhancement of the dimer was estimated, a series of experiments to determine the highest concentrations at which a single fluorophore could be detected were performed. For this purpose two samples were prepared, a dimer structure and a DNA origami nanopillar without NPs. Confocal fluorescence images and transients were recorded while increasing the background concentration. The same fluorophore, ATTO647N, was employed for the background. Figure 4 shows a confocal image of the sample without NPs (a) with no added background and (b) with a background of 4 nM. As expected, by increasing the background concentration, the image gets less sharp and single spots become more difficult to be resolved. Increasing the concentration further than 4 nM prevented single fluorophores from being identified. The corresponding images for the dimer sample are included in Fig. 4(c) and 4(d) for no background and 500 nm, respectively.

In addition to the confocal images, fluorescence transients were recorded. Figure 5 shows the corresponding transients for the nanopillar (a) without NP and no background and (b) with a 4-nM background. While the blinking steps are of comparable magnitude, the transient with background is noisier and shows an "offset" due to the presence of the fluorophores in the background. The fluorescence decays are included in Fig. 5(c) and yield a monoexponential decay of 3.8 ns typical for ATTO647N. The corresponding transients for the dimer sample are presented in Fig. 5(d) and 5(e). The dimer sample exhibits blinking steps which are still clearly resolvable at concentrations more than 2 orders of magnitude higher than for the sample with no NPs. Furthermore, the fluorescence decay for the dimer with a background concentration of 500 nM [Fig. 5(f)] shows a biexponential decay, due to the combination of an enhanced single fluorophore at the hotspot interacting with the NPs and the background of fluorophores within the diffraction-limited volume. The shorter decay of the fluorophore in the hotspot indicates the possibility of further signal-to-noise improvement by time-gating.[14]
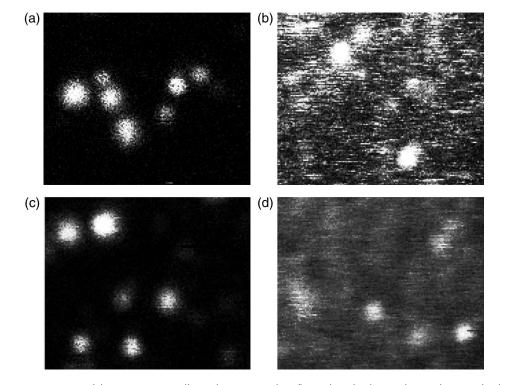

Fig. 4 Confocal fluorescence image of the origami nanopillar without NPs and no fluorophore background (a) and a 4 nM background (b). (c) and (d) Dimer sample with no background and 500 nM of fluorophore background, respectively.
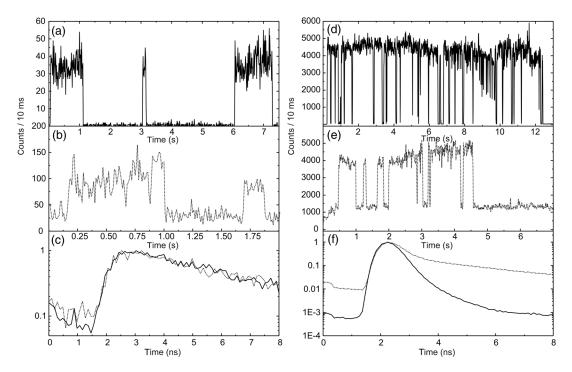
Fig. 5 Fluorescence transient of the DNA origami nanopillar without NPs and no fluorophore background (a) and a 4 nM background (b). (c) Corresponding lifetime decays. (d) and (e) Dimer sample with no background and 500 nM of fluorophore background, respectively and (f) fluorescence lifetime decay.

5   Conclusions

We have employed the recently developed DNA-origami technique to build nanoantennas formed by two 100 nm gold NPs. The spacing between the particles of 23 nm was chosen to host biomolecular assays. These structures can focus the electric field to a reduced hotspot and yield fluorescence enhancement of up to 2 orders of magnitude. The nanoantenna dimers were also employed to extend the concentration at which a single fluorophore can be detected from 4 to 500 nM.

References

1. T. A. Laurence and S. Weiss, "Analytical chemistry. How to detect weak pairs," *Science* **299**(5607), 667–668 (2003).
2. K. T. Samiee et al., "Lambda-repressor oligomerization kinetics at high concentrations using fluorescence correlation spectroscopy in zero-mode waveguides," *Biophys. J.* **88**(3), 2145–2153 (2005).
3. J. M. Moran-Mirabal and H. G. Craighead, "Zero-mode waveguides: sub-wavelength nanostructures for single molecule studies at high concentrations," *Methods* **46**(1), 11–17 (2008).
4. M. J. Levene et al., "Zero-mode waveguides for single-molecule analysis at high concentrations," *Science* **299**(5607), 682–686 (2003).
5. L. Novotny and N. van Hulst, "Antennas for light," *Nat. Photon.* **5**, 83–90 (2011).
6. A. Kinkhabwala et al., "Large single-molecule fluorescence enhancements produced by a bowtie nanoantenna," *Nat. Photon.* **3**, 654–657 (2009).
7. A. Kinkhabwala et al., "Fluorescence correlation spectroscopy at high concentrations using gold bowtie nanoantennas," *Chem. Phys.* **406**, 3–8 (2012).
8. P. W. Rothemund, "Folding DNA to create nanoscale shapes and patterns," *Nature* **440**(7082), 297–302 (2006).
9. B. Ding et al., "Gold nanoparticle self-similar chain structure organized by DNA origami," *J. Am. Chem. Soc.* **132**(10), 3248–3249 (2010).
10. P. Anger, P. Bharadwaj, and L. Novotny, "Enhancement and quenching of single-molecule fluorescence," *Phys. Rev. Lett.* **96**(11), 113002 (2006).
11. S. Kuhn et al., "Enhancement of single-molecule fluorescence using a gold nanoparticle as an optical nanoantenna," *Phys. Rev. Lett.* **97**(1), 017402 (2006).
12. E. A. Coronado, E. R. Encina, and F. D. Stefani, "Optical properties of metallic nanoparticles: manipulating light, heat and forces at the nanoscale," *Nanoscale* **3**(10), 4042–4059 (2011).
13. M. I. Stockman, "Nanoplasmonics: past, present, and glimpse into future," *Opt. Express.* **19**(22), 22029–22106 (2011).
14. G. P. Acuna et al., "Fluorescence enhancement at docking sites of DNA-directed self-assembled nanoantennas," *Science* **338**(6106), 506–510 (2012).
15. J. J. Schmied et al., "DNA origami nanopillars as standards for three-dimensional superresolution microscopy," *Nano Lett.* **13**(2), 781–785 (2013).
16. C. A. Mirkin et al., "A DNA-based method for rationally assembling nanoparticles into macroscopic materials," *Nature* **382**(6592), 607–609 (1996).
17. G. P. Acuna et al., "Distance dependence of single-fluorophore quenching by gold nanoparticles studied on DNA origami," *ACS Nano* **6**(4), 3189–3195 (2012).
18. J. Vogelsang et al., "A reducing and oxidizing system minimizes photobleaching and blinking of fluorescent dyes," *Angew. Chem. Int. Ed.* **47**(29), 5465–5469 (2008).